Supporting Information

A report on Se/Eu-doped hydroxyapatite: crystal structure analysis, biological property assessment, and applications in osteosarcoma inhibition and bioimaging

Shuoshuo Zhou [a,b,1]，Jian Ren [a,b,1], Lunzhu Wang [a,b], Liting Liu [a,b], Chunlin Deng [a,b,c,*]

[a] School of Materials Science and Engineering, South China University of Technology, Guangzhou 510641, China.

[b] National Engineering Research Center for Tissue Restoration and Reconstruction, Guangzhou 510006, China.

[c] Key Laboratory of Biomedical Engineering of Guangdong Province, South China University of Technology, Guangzhou 510006, China.

[1] These authors contributed equally to this study and should be considered co-first authors

* Corresponding Authors:

E-mail: chldeng@ scut.edu.cn

Table S1 R values (including R_{wp}, R_p, χ^2, for evaluate refined fit parameters) and crystal structure parameters of HAp and HAp-Se samples obtained by Rietveld refinement.

Sample	Rwp (%)	Rp(%)	χ^2	Lattice Parameters: a&b(Å)	Lattice Parameters :c(Å)	Volume of cell (Å³)	Density (g/cm³)	Average bond length(Å)				
								Ca-Ca	Ca-P	Ca-Se	Ca-O	P-O
HAp	3.540	2.580	2.511	9.427	6.877	529.339	3.139	3.963	3.359	-	2.519	1.519
HAp-1%Se	3.040	2.300	1.925	9.429	6.878	529.511	3.396	3.980	3.356	3.413	2.527	1.518
HAp-3%Se	3.160	2.380	2.007	9.431	6.879	529.879	3.326	3.978	3.361	3.417	2.523	1.520
HAp-5%Se	2.910	2.240	1.824	9.432	6.878	529.912	3.302	3.981	3.359	3.415	2.525	1.513
HAp-8%Se	2.930	2.250	1.764	9.436	6.877	530.302	3.225	3.982	3.360	3.416	2.522	1.521
HAp-10%Se	3.090	2.350	2.047	9.434	6.882	530.354	3.290	3.980	3.361	3.418	2.515	1.542

Table S2 Atomic parameters of HAp and HAp-Se samples obtained by Rietveld refinement

Sample	Atomic parameters	Atom type						
		Ca I	Ca II	P	Se	O I	O II	O III
HAp	x	0.333	0.247	0.401	-	0.326	0.582	0.340
	y	0.667	0.990	0.371	-	0.481	0.463	0.255
	z	0.002	0.250	0.250	-	0.250	0.250	0.074
	Occupancy	1.023	1.036	0.961	-	0.992	0.960	0.969
HAp-1%Se	x	0.333	0.248	0.402	0.402	0.326	0.584	0.335
	y	0.667	0.990	0.373	0.373	0.482	0.464	0.255
	z	0.003	0.250	0.250	0.250	0.250	0.250	0.076
	Occupancy	1.070	1.036	0.996	0.004	1.091	1.063	1.155
HAp-3%Se	x	0.333	0.246	0.400	0.400	0.326	0.586	0.339
	y	0.667	0.991	0.371	0.371	0.484	0.468	0.258
	z	0.002	0.250	0.250	0.250	0.250	0.250	0.076
	Occupancy	1.017	1.034	0.987	0.013	1.039	1.047	1.122
HAp-5%Se	x	0.333	0.247	0.401	0.401	0.326	0.583	0.338
	y	0.667	0.990	0.372	0.372	0.482	0.466	0.256
	z	0.002	0.250	0.250	0.250	0.250	0.250	0.077
	Occupancy	1.025	1.028	0.965	0.035	1.029	1.020	1.072
HAp-8%Se	x	0.333	0.248	0.401	0.401	0.327	0.582	0.339
	y	0.667	0.990	0.372	0.372	0.483	0.463	0.256
	z	0.002	0.250	0.250	0.250	0.250	0.250	0.074
	Occupancy	0.988	1.000	0.957	0.043	1.080	0.983	0.996
HAp-10%Se	x	0.333	0.246	0.400	0.400	0.326	0.585	0.339
	y	0.667	0.990	0.371	0.371	0.483	0.467	0.254
	z	0.001	0.250	0.250	0.250	0.250	0.250	0.071
	Occupancy	1.002	1.009	0.927	0.073	1.036	1.013	1.061

In order to learn more about the impact of selenium doping on HAp, Rietveld refinement

was performed on HAp-Se (0%, 1%, 3%, 5%, 8%, 10%) samples with the aid of the GSAS program. The initial setting was Se occupying position P, while Tables S1 and S2 display the refined reliability parameters, lattice parameters, bond length parameters, atomic coordinates, and occupancy. In Table S1, $R_{wp} < 5\%$ and $\chi^2 < 3\%$ show that the refinement results are highly reliable. The lattice constants a, c, unit cell volume, and interatomic bond length of HAp tend to increase with an increase in Se doping level. This is because SeO_3^{2-} was partially substituted for the PO_4^{3-} position. The Se ion radius (0.05 nm) is larger than the P ion radius (0.038 nm), and the volume of the SeO_3^{2-} trigonal cone is larger than the PO_4^{3-} tetrahedral volume, the mismatch in size and shape causes the lattice distortion[15]. Table S2 displays the atomic positions and occupancy of samples with Se doping. From the perspective of atomic occupancy, the actual atomic percentage of selenium is roughly half of the theoretical value, showing that Se is only partially absorbed into the lattice. From the perspective of atomic coordinates, Se doping has little impact on other atoms. The Se-doped HAp has a lower proportion of Ca than the undoped samples, which is owing to a decrease in Ca^{2+} concentration brought on by charge compensation[15] when part of the PO_4^{3-} is partially replaced by SeO_3^{2-}.
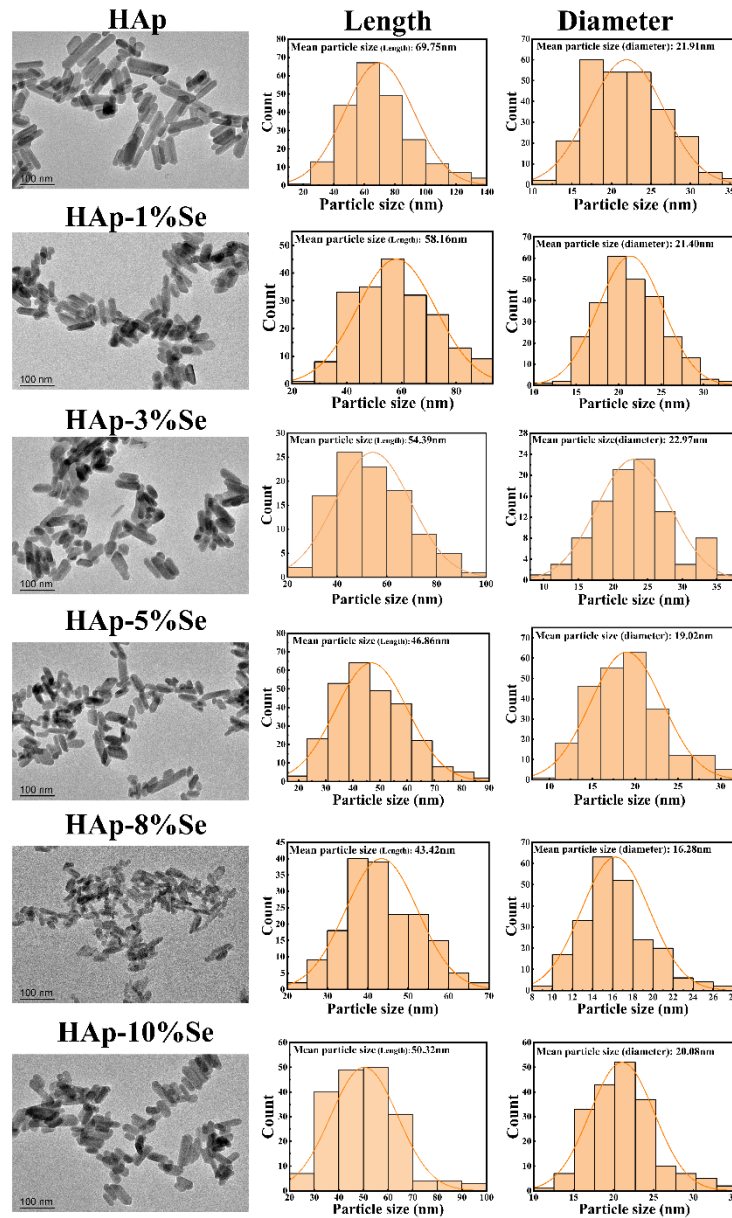
Figure S1 TEM images and particle size distribution of HAp and HAp-Se samples (length & diameter)

Figure S1 illustrates the TEM morphology and the particle length and diameter distribution of HAp-Se (0%, 1%, 3%, 5%, 8%, and 10%) samples. According to the morphology, Se doping caused the nanoparticles change from thicker and longer rods to thinner and shorter rods, and the degree of agglomeration of the nanoparticles increased. According to the particle size distribution curve, the average particle size tended to gradually decrease with an increase in Se doping, and it reached its smallest size in HAp-8%Se, with an average length and diameter of 46.86nm and 19.02nm. The size distribution of the HAp-8%Se sample is narrower than that of the other samples.

Table S3 R values (including R_{wp}, R_p, χ^2, for evaluate refined fit parameters) and crystal structure parameters of HAp and HAp-Eu samples obtained by Rietveld refinement.

Sample	Rwp (%)	Rp (%)	χ^2	Phase 1:HAp					Phase 2:EuP5O14					
				Fraction（wt）	Lattice Parameters		Volume of cell (Å³)	Density (g/cm³)	Fraction（wt）	Lattice Parameters			Volume of cell (Å³)	Density (g/cm³)
					a&b	c				a	b	c		
HAp	3.540	2.580	2.511	1.000	9.427	6.877	529.339	3.139	0.000	-	-	-	-	-
HAp-5%Eu	2.370	1.830	1.224	0.799	9.431	6.880	529.926	3.314	0.201	8.157	8.718	14.366	1021.625	7.364
HAp-10%Eu	2.370	1.860	1.871	0.769	9.428	6.882	529.750	3.494	0.231	8.053	8.185	14.968	1062.777	5.930
HAp-15%Eu	2.120	1.660	1.219	0.693	9.426	6.882	529.515	3.661	0.307	9.970	8.574	13.407	1142.729	3.930
HAp-20%Eu	2.090	1.660	1.187	0.709	9.417	6.880	528.432	3.816	0.290	9.321	8.674	13.019	1044.243	4.258

Table S4 Atomic parameters of HAp and HAp-Eu samples obtained by Rietveld refinement

Sample	Atomic parameters	Atom type							
		Ca I	Ca II	Eu I	Eu II	P	O I	O II	O III
HAp	x	0.333	0.247	-	-	0.401	0.326	0.582	0.340
	y	0.667	0.990	-	-	0.371	0.481	0.463	0.255
	z	0.002	0.250	-	-	0.250	0.250	0.250	0.074
	Occupancy	1.023	1.036	-	-	0.961	0.992	0.960	0.969
HAp-5%Eu	x	0.333	0.248	0.333	0.248	0.393	0.323	0.589	0.327
	y	0.667	0.989	0.667	0.989	0.368	0.484	0.457	0.263
	z	0.005	0.250	0.005	0.250	0.250	0.250	0.250	0.064
	Occupancy	0.978	0.970	0.022	0.030	0.902	1.109	1.354	1.169
HAp-10%Eu	x	0.333	0.246	0.333	0.246	0.398	0.345	0.596	0.334
	y	0.667	0.990	0.667	0.990	0.371	0.487	0.471	0.252
	z	0.004	0.250	0.004	0.250	0.250	0.250	0.250	0.077
	Occupancy	0.918	0.918	0.082	0.082	1.017	1.071	1.069	1.124
HAp-15%Eu	x	0.333	0.243	0.333	0.243	0.402	0.333	0.565	0.320
	y	0.667	0.975	0.667	0.975	0.375	0.464	0.428	0.250
	z	0.011	0.250	0.011	0.250	0.250	0.250	0.250	0.057
	Occupancy	0.907	0.854	0.093	0.146	0.939	1.008	1.187	0.901
HAp-20%Eu	x	0.333	0.225	0.333	0.225	0.423	0.308	0.542	0.331
	y	0.667	0.992	0.667	0.992	0.360	0.495	0.461	0.269
	z	0.004	0.250	0.004	0.250	0.250	0.250	0.250	0.057
	Occupancy	0.859	0.832	0.141	0.169	1.026	1.089	1.090	1.007

With initial settings of Eu occupying Ca, HAp as the first phase, and EuP_5O_{14} as the second phase, Rietveld refinement was carried out on HAp-Eu (0%, 5%, 10%, 15%, 20%) samples using GSAS software. The reliability parameters, cell parameters, atomic coordinates, and occupancy obtained from the refinement are shown in Tables S3 and S4, which showed $R_{wp}<$

5% and $\chi^2 < 3\%$, meaning the findings of the refinement are highly reliable. Table S3 demonstrates that as the Eu doping content increases, the HAp phase content decreases and then increases, while the cell parameter increases and then decreases. The larger cell parameter may be connected to the formation of the EuP_5O_{14} phase. And as the Eu doping content rises, the substitution of the smaller ionic radius Eu^{3+} (0.095 nm) for the larger ionic radius Ca^{2+} (0.099 nm) in HAp decreases the lattice constant a and c[29]. The atomic positions and occupancies of the HAp-Eu samples are displayed in Table S4. The atomic occupancy ratio demonstrates that Eu is successfully doped into the HAp lattice by occupying the atomic coordinates of Ca, but the actual atomic occupancy ratio of Eu is smaller than the theoretical value, indicating that a small amount of Eu exists in the form of the EuP_5O_{14} phase. In addition, the ratio of each atom of PO_4^{3-} in HAp displays a trend of sawtooth fluctuation with the doping content changing, which may be caused by combination of charge compensation as well as the second phase.
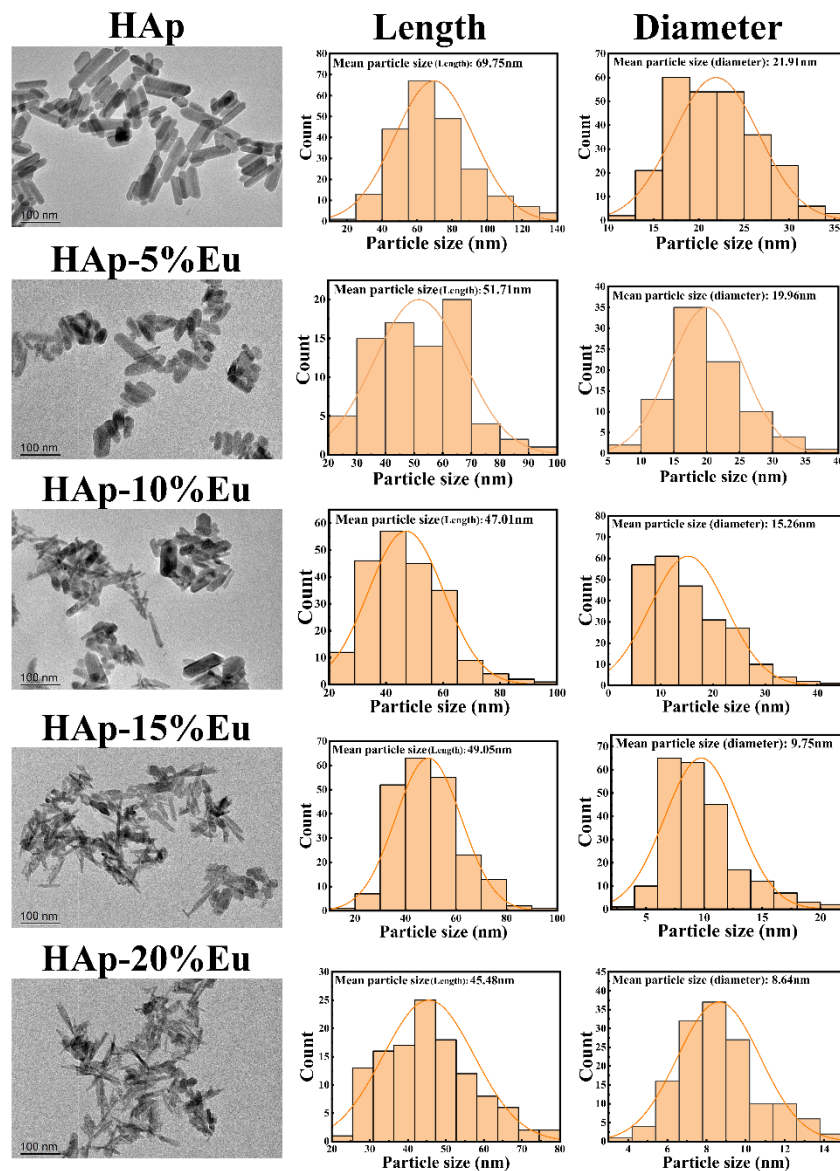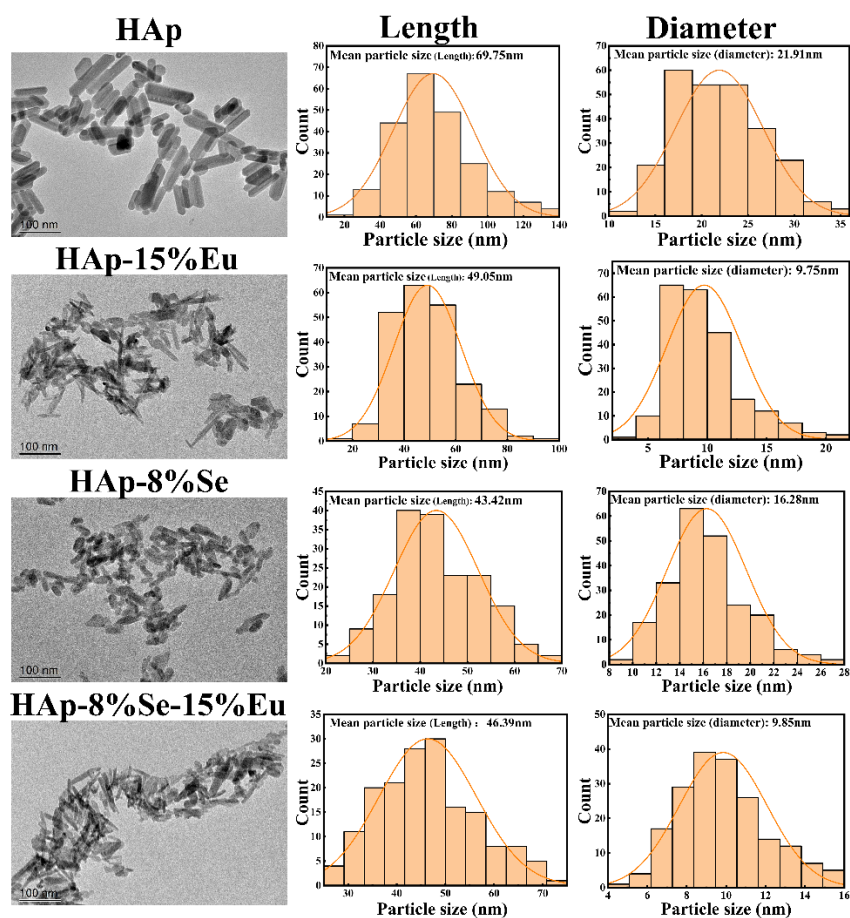
Figure S2 TEM images and particle size distribution of HAp and HAp-Eu samples (length & diameter)

Figure S2 shows the TEM morphology and the particle length and diameter distribution of HAp-Eu (0%, 5%, 10%, 15%, 20%). The morphology of the material is greatly influenced by Eu doping content. As the Eu doping content increases, the particle size decreases noticeably and a needle-like morphology gradually appears. The size distribution of the material also becomes unbalanced, and material aggregation worsens, which may be related to the post-doping heterogeneous phase EuP_5O_{14} synthesis.

Figure S3 TEM images and particle size distribution of samples (length & diameter)

Figure S3 displays the TEM morphology and the particle length and diameter distribution of the HAp, HAp-8%Se, HAp-15%Eu, and HAp-8%Se-15%Eu samples. Se doping had a slight impact on length and diameter, converting the material from thicker long rods to thinner short rods. Eu doping greatly reduced the diameter of the material, presenting needle-like morphology, and the particle size distribution was rather uneven. However, co-doping reduces the needle-like morphology and makes the size distribution more homogeneous than single Eu-doping, though material agglomeration still occurs.
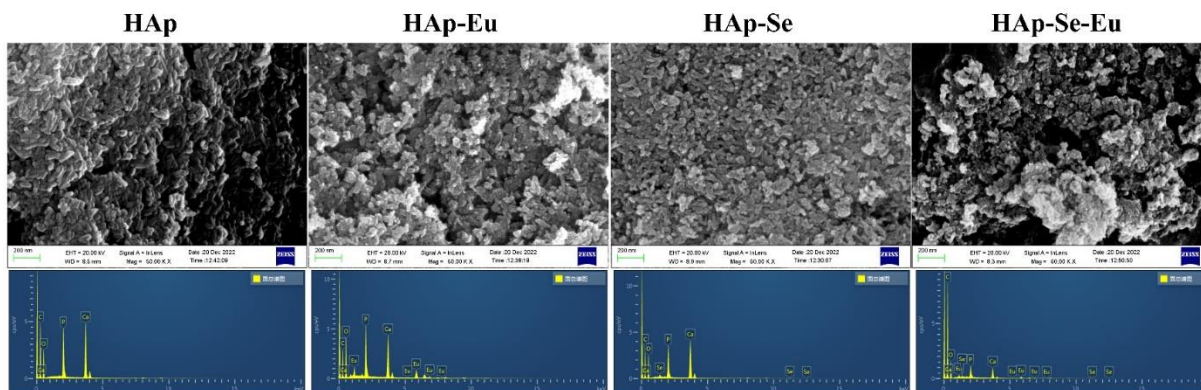
Figure S4 SEM morphology of the samples

Figure S4 depicts the SEM morphology of the samples. All samples are rod-shaped, with the most complete morphology being HA. Se doping has little effect on the morphology of the materials, whereas Eu doping makes the material rod-shaped shorter and thinner, and more agglomeration, which is consistent with the TEM results. Furthermore, the non-rod-shaped particles on the surface of the Eu-containing materials may be the new phase, which is sparsely distributed on the sample's surface and has a lower percentage. The main body of the sample is still in the HA phase, as indicated by the XRD results.
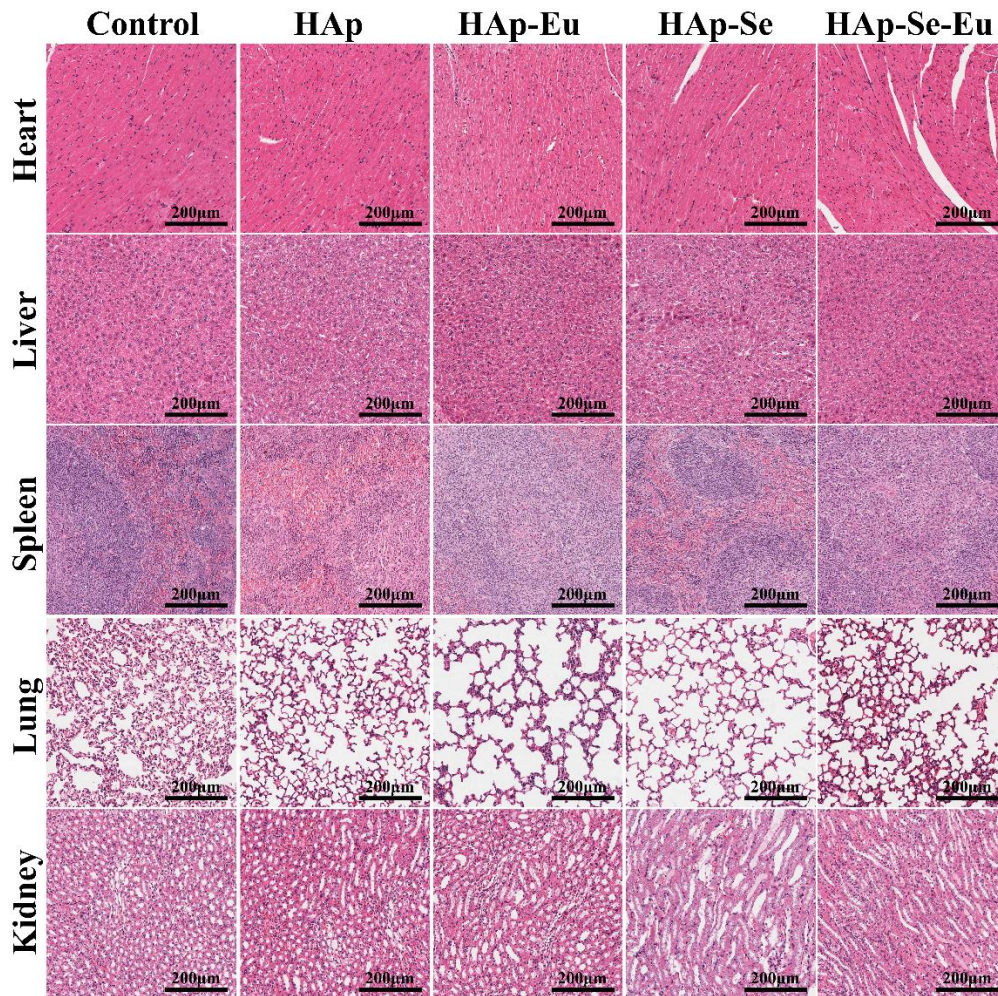
Figure S5 H&E staining of major organs of mice treated with different samples

As shown in Figure S5, the tissue structures of several major organs were relatively intact, with uniform cell coloring, distinct cell boundaries, and basically consistent cell morphology, devoid of obvious lesion features. The cardiomyocytes were arranged neatly. The structure of the hepatic lobules was normal, and the hepatic cords were neatly arranged. Blood vessels and lymphatic tissues were interspersed throughout the spleen. The lung cavity was alveolar with a distinct outline. The glomerulus with complete structure and the renal tubules were neatly arranged in the kidney tissue. These findings demonstrated that nanomaterials did not cause organ damage or abnormalities in mice and could be used to inhibit the growth of osteosarcoma while remaining biologically safe.